Geophysical Research Letters

RESEARCH LETTER
10.1029/2023GL105208

Tracing Subducted Carbonates in Earth's Mantle Using Zinc and Molybdenum Isotopes

Jian Wang[1,2], Gong-Jian Tang[1], Sebastian Tappe[3], Jie Li[1], Zongqi Zou[1,2], Qiang Wang[1], Yu-Ping Su[2], and Jian-Ping Zheng[2]

[1]State Key Laboratory of Isotope Geochemistry, Guangzhou Institute of Geochemistry, Chinese Academy of Sciences, Guangzhou, China, [2]State Key Laboratory of Geological Processes and Mineral Resources, School of Earth Sciences, China University of Geosciences, Wuhan, China, [3]Department of Geosciences, UiT—The Arctic University of Norway, Tromsø, Norway

Key Points:

- First combined zinc (Zn) and molybdenum (Mo) isotope data for mantle-derived magmas to track the fate of subducted carbonates
- Zn–Mo isotopic compositions of Cenozoic Tarim basalts suggest surficial carbonates being delivered into the deep upper mantle
- We highlight the utility of combined Zn–Mo isotope data as a powerful tool in deep carbon science

Supporting Information:

Supporting Information may be found in the online version of this article.

Correspondence to:

G.-J. Tang,
tanggj@gig.ac.cn

Citation:

Wang, J., Tang, G.-J., Tappe, S., Li, J., Zou, Z., Wang, Q., et al. (2024). Tracing subducted carbonates in Earth's mantle using zinc and molybdenum isotopes. *Geophysical Research Letters*, *51*, e2023GL105208. https://doi.org/10.1029/2023GL105208

Received 28 JUN 2023
Accepted 7 FEB 2024

Author Contributions:

Conceptualization: Jian Wang
Funding acquisition: Gong-Jian Tang, Qiang Wang
Investigation: Yu-Ping Su, Jian-Ping Zheng
Methodology: Jian Wang, Jie Li
Project administration: Gong-Jian Tang
Supervision: Gong-Jian Tang, Qiang Wang
Writing – original draft: Jian Wang
Writing – review & editing: Gong-Jian Tang, Sebastian Tappe, Zongqi Zou

Abstract Although carbonates are the primary form of carbon subducted into the mantle, their fate during recycling is debated. Here we report the first coupled high-precision Zn and Mo isotope data for Cenozoic intraplate basalts from western China. The exceptionally high δ^{66}Zn values (+0.39 to +0.50‰) of these lavas require involvement of recycled carbonates in the mantle source. Variable δ^{98}Mo compositions (−0.39 to +0.27‰) are positively correlated with Mo/Ce, best interpreted as mixing between isotopically light Mo from dehydrated oceanic crust and heavy Mo from recycled carbonates, which is also supported by positive coupling between δ^{66}Zn and δ^{98}Mo. Modeling reveals that involvement of ≤5% carbonate-bearing oceanic crust fully resolves the observed δ^{66}Zn–δ^{98}Mo mantle heterogeneity probed by intracontinental basalts. Our study demonstrates that combined δ^{66}Zn–δ^{98}Mo data sets for mantle-derived magmas can track recycled surficial carbonates in Earth's interior, providing a powerful geochemical tool for deep carbon science.

Plain Language Summary Carbon is an element of life and studying its geological cycle is crucial for understanding Earth's evolution including formation of a life-supporting atmosphere. Here we report the first combined high-precision Zn and Mo isotope data for Cenozoic intraplate lavas from western China, showing that the basalts record ≤5% carbonate-bearing oceanic crust components in their mantle source. Our results provide new evidence for surficial carbonates being delivered into the deep upper mantle, which adds to the debate about the deepest extent of the terrestrial carbon cycle.

1. Introduction

Cycling of carbon between Earth's surface and interior plays a key role in regulating climate and maintaining a habitable planet. Carbon at the Earth's surface is present mainly as sedimentary carbonates, which can be transported into the mantle by subduction of oceanic lithosphere. However, the fate of subducted carbonates remains poorly understood. Although carbon isotopes are effective in identifying recycled organic carbon at mantle depths (Smart et al., 2011), the δ^{13}C values of mantle-derived materials cannot always unambiguously distinguish between primordial and recycled inorganic carbon sources such as sedimentary carbonates (Deines, 2002). Some authors propose that almost all carbon is liberated from subducting slabs and transferred into the subarc mantle mainly because of the high carbon solubility in aqueous fluids, with the implication that only little subducted carbon (as low as 0.0001 Mt C/yr) reaches the deep mantle (Kelemen & Manning, 2015). In contrast, some experiments demonstrate that carbonate minerals can be preserved in subducting slabs under high P-T conditions, with the prediction that about half of the subducting carbon (24–48 Mt C/yr) can enter the deep upper mantle and beyond (Dasgupta et al., 2004). The compositions of superdeep diamonds and their inclusions provide evidence for the recycling of surficial carbon down to 800 km depth (Smith et al., 2018; Walter et al., 2011). However, the low-δ^{13}C signatures of such sublithospheric diamonds imply recycled organic matter rather than sedimentary carbonates as the original carbon source (Walter et al., 2011).

Zinc (Zn) and molybdenum (Mo) isotopes have great potential to address the above controversy, because (a) marine carbonates are characterized by significantly heavier δ^{66}Zn (+0.91 ± 0.54‰, n = 171) and δ^{98}Mo (+1.66 ± 1.02‰, n = 62) values than those accepted as normal mantle compositions (+0.16 ± 0.06‰ δ^{66}Zn and −0.20 ± 0.01‰ δ^{98}Mo) (Figure 2); (b) the two stable isotope tracers show limited fractionation during partial melting and magma ascent (Bezard et al., 2016; Day et al., 2022; Wang et al., 2017), and (c) Mo exhibits higher mobility compared to Zn and can be efficiently transported by slab fluids into subarc mantle wedge environments.

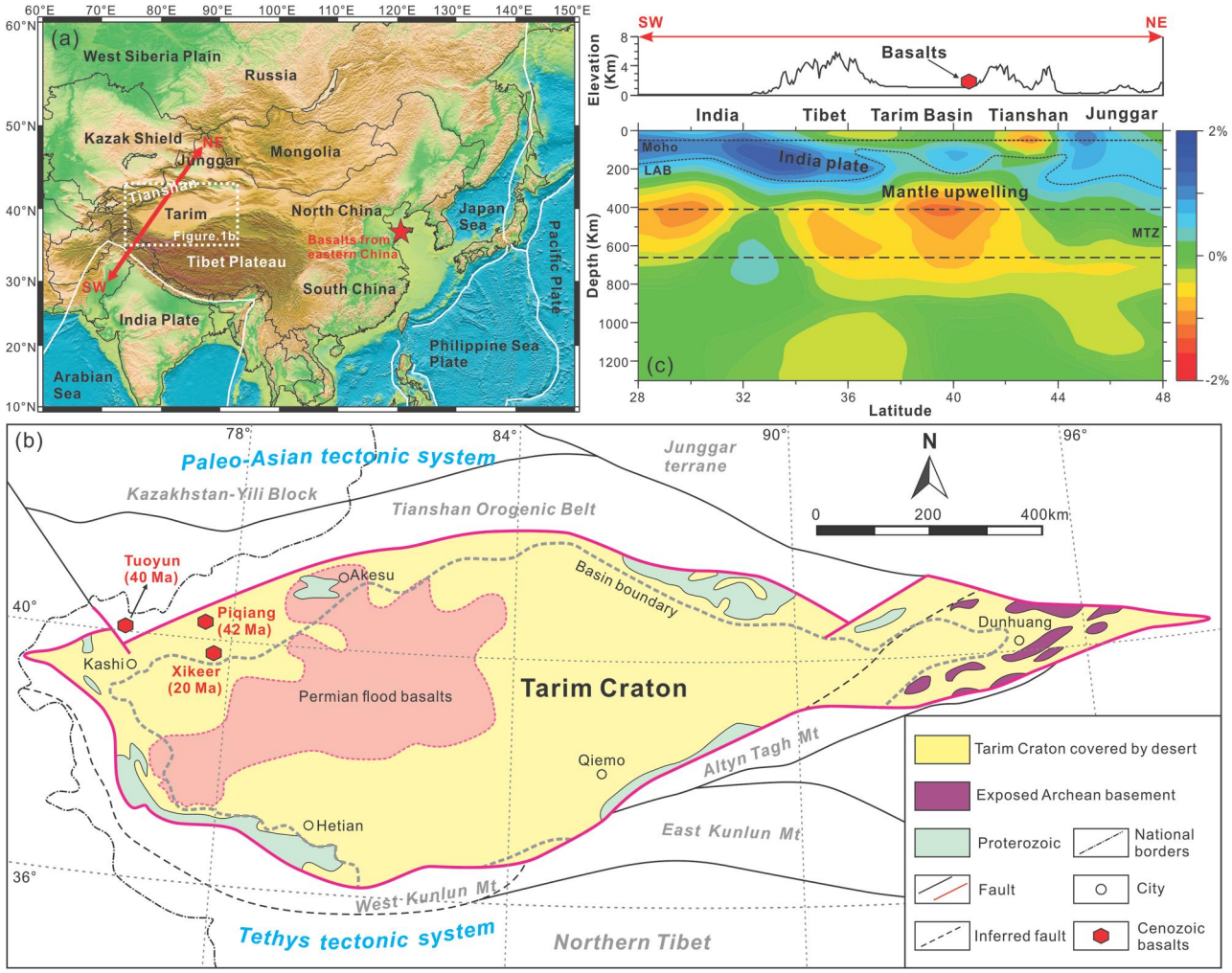

Figure 1. (a) Map of the central Asian continent with major geological blocks and plate boundaries. The red line (SW-NE) is the profile shown in panel c. Cenozoic basalts with available Zn-Mo isotopic data from the Shandong Peninsula, eastern China are shown for comparison (X. J. Wang et al., 2018; Z. Z. Wang et al., 2018; Li et al., 2019). (b) Geological map of the Tarim Craton and surroundings. Cenozoic basalts in this study were sampled from the NW Tarim, including Tuoyun, Piqiang and Xiker. (c) Surface topography and vertical cross-section P-wave tomography along the profile (SW-NE) in panel a (after Huang & Zhao, 2006).

The Mo isotope system has been widely used in tracing the recycling of crustal materials in subduction zones, and, thus may provide additional insights into the geochemical behavior of subducting carbon during slab dehydration (Fang et al., 2023; König et al., 2016; Zhang et al., 2020). Hence, it can be assumed that basaltic magmas sourced from mantle domains that have been refertilized by recycled carbonates should have higher δ^{66}Zn and δ^{98}Mo compositions compared to magmas derived from "normal" or more depleted mantle reservoirs.

To test this hypothesis, we present the first combined δ^{66}Zn–δ^{98}Mo data set for Cenozoic basalts from western China. Integrating the new data with δ^{66}Zn–δ^{98}Mo data for Cenozoic basalts from eastern China and δ^{66}Zn data from western China (X. J. Wang et al., 2018; Z. Z. Wang et al., 2018; Li et al., 2019; Cheng et al., 2022), we show that involvement of ≤5% carbonate-bearing oceanic crust in the mantle source can reconcile the heavy Zn–Mo isotopic signatures of these intracontinental basalts. Our study provides evidence for surficial carbonates being delivered into the deeper convecting upper mantle, highlighting the importance of subduction-driven deep carbon cycling.

2. Geological Setting, Samples, and Results

The Tarim Craton in western China is bound by the Tianshan and Kunlun orogenic belts to the north and south respectively (Figure 1). The craton comprises early Archean to Neoproterozoic crystalline basement rocks largely

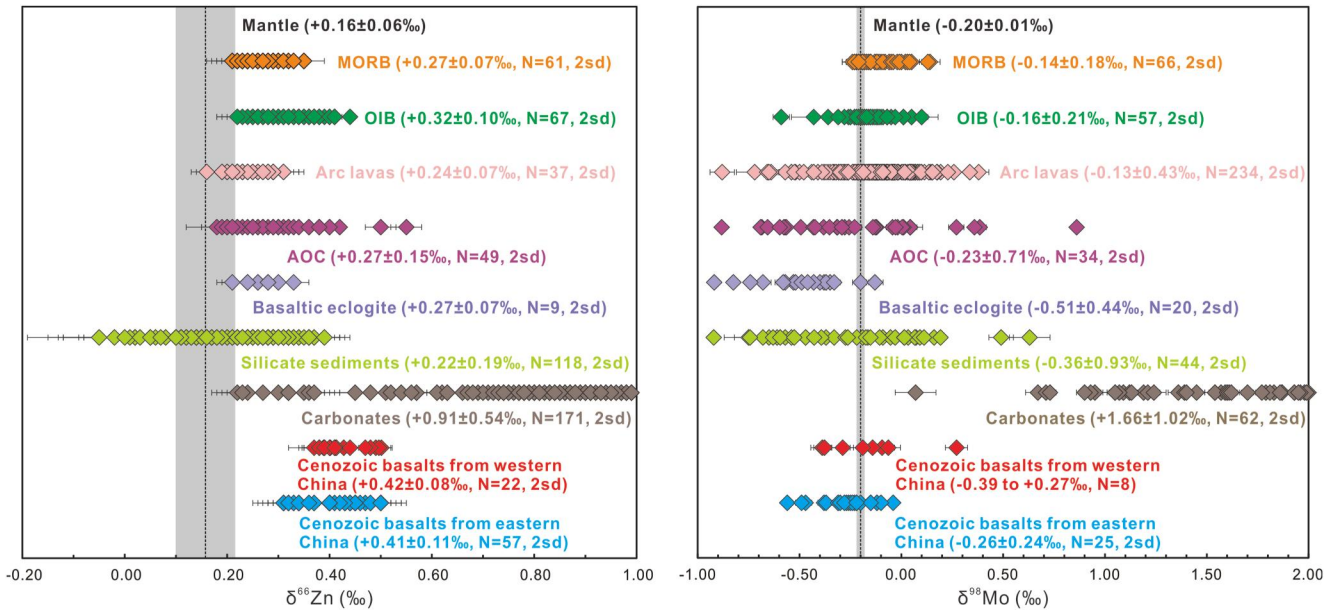

Figure 2. δ^{66}Zn and δ^{98}Mo isotope compositions of Cenozoic basalts from western and eastern China (Cheng et al., 2022; Li et al., 2019; X. J. Wang et al., 2018; Z. Z. Wang et al., 2018 and this study). The mantle δ^{66}Zn and δ^{98}Mo are from Sossi et al. (2018) and McCoy-West et al. (2019). Also shown for comparison include MORB (δ^{66}Zn: Day et al., 2022; Pickard et al., 2022; Sun et al., 2023; Wang et al., 2017; δ^{98}Mo: Bezard et al., 2016; Chen et al., 2022; Liang et al., 2017), OIB (δ^{66}Zn: Chen et al., 2013; Pickard et al., 2022; Wang et al., 2017; Zhang et al., 2022; δ^{98}Mo: Bezard et al., 2016; Gaschnig et al., 2021; Liang et al., 2017; Yang et al., 2015), arc lavas (δ^{66}Zn: Huang et al., 2018; δ^{98}Mo: Ahmad et al., 2021; Fang et al., 2023; Freymuth et al., 2015, 2016; Gaschnig et al., 2017; König et al., 2016; Li, Zhao, et al., 2021; Li, Yan, et al., 2021; Villalobos-Orchard et al., 2020; Yu et al., 2022), AOC (δ^{66}Zn: Huang et al., 2016; δ^{98}Mo: Ahmad et al., 2021; Freymuth et al., 2015), basaltic eclogites (δ^{66}Zn: Inglis et al., 2017; δ^{98}Mo: Ahmad et al., 2021; Chen et al., 2019), silicate sediments (δ^{66}Zn: Little et al., 2016; Maréchal et al., 2000; Qu et al., 2022; Sonke et al., 2008; Vance et al., 2016; δ^{98}Mo: Ahmad et al., 2021; Freymuth et al., 2015; Gaschnig et al., 2017) and carbonates (δ^{66}Zn: Pichat et al., 2003; Liu et al., 2017; Sweere et al., 2018; δ^{98}Mo: Lin et al., 2021; Romaniello et al., 2016; Voegelin et al., 2009).

covered by Phanerozoic sedimentary rocks. After closure of the Paleo-Tethys Ocean at ~220 Ma, the wider Tarim Craton region transitioned into a stable intracontinental setting that was not affected by major magmatic events until the India−Eurasia collision at ~50 Ma. Our study utilizes young primitive olivine-phyric basalts from the NW Tarim, including sampling sites at Tuoyun (~40 Ma), Piqiang (~42 Ma) and Xiker (~20 Ma) (Figure S2 in Supporting Information S1). Recent studies suggest that these Cenozoic basaltic magmas were derived from the asthenospheric mantle, possibly related to collision-induced mantle upwelling (Wang et al., 2023). For more details about the geological setting and samples, readers are referred to the Supporting Information S1.

Representative basalt samples were selected for major-trace element analyses, and for Sr-Nd-Pb-Zn-Mo isotope ratio determinations (see Supporting Information S1 for detailed descriptions of methods and results). The samples analyzed are typical intracontinental alkali basalts characterized by incompatible trace-element enrichment and moderately depleted Sr-Nd-Pb isotopic compositions (Figures S3 and S4 in Supporting Information S1). They have δ^{66}Zn values of +0.39 to +0.50 ‰ at 91.2–128 ppm Zn and 10.9–15.5 Zn/Fe as mantle lithology proxy (Figure 2, Le Roux et al., 2010). The δ^{98}Mo compositions range from −0.39 to +0.27‰ at 2.26–7.16 ppm Mo and 0.04–0.08 Mo/Ce (Figure 2). The Tarim basalts of western China are geochemically very similar to their Cenozoic analogs from eastern China, although the former has more of an EM2 signature than the latter (Figures S3 and S4 in Supporting Information S1).

3. Discussion

The Zn and Mo isotopic signatures of the Tarim basalts are either inherited from the mantle source or they developed during shallow-level magmatic processes. The δ^{66}Zn and δ^{98}Mo values show no systematic variations with loss on ignition, indicating that alteration and weathering effects are negligible (Figure S6 in Supporting Information S1). Significant crustal contamination can be ruled out because the samples have depleted Sr-Nd-Pb isotopic compositions, positive Nb−Ta anomalies, and high Nb/U and Ce/Pb ratios (Figures S3–S5 in Supporting Information S1). The basalts studied have primitive elemental compositions (6.8–12.8 wt.% MgO), implying that

olivine and Cr-spinel are the main liquidus phases. However, there are no correlations between δ^{66}Zn–δ^{98}Mo values and Ni or Cr contents (Figure S6 in Supporting Information S1), which rules out resolvable isotopic fractionation along a liquid line of descent. Partial melting has been proposed as a key factor controlling the Zn isotopic compositions of basalts (Day et al., 2022; Doucet et al., 2016), which is supported by the positive correlations between δ^{66}Zn and La/Sm (proxy for the degree of partial melting) in our sample suite (Figure S6 in Supporting Information S1). Doucet et al. (2016) suggest that partial melting of fertile mantle peridotite in excess of 30% may increase δ^{66}Zn in the resultant melts by up to 0.16‰. However, the alkali basalts studied formed by much lower degrees of partial melting (<10%) (Wang et al., 2023), and they have much higher δ^{66}Zn of up to +0.50‰ compared to normal mantle (up to +0.34‰). This suggests that partial melting alone cannot explain the high δ^{66}Zn measured. On the basis of this evidence and the lack of correlation between δ^{98}Mo and La/Sm (Figure S6 in Supporting Information S1), we conclude that the δ^{66}Zn–δ^{98}Mo compositions of the Tarim basalts are inherited mainly from their mantle source.

Basaltic magmas derived from a volatile-poor peridotite source typically have <0.30‰ δ^{66}Zn (Wang et al., 2017). Thus, the exceptionally high δ^{66}Zn (+0.39 to +0.50‰, Figure 2) of the Tarim basalts is best explained by involvement of ^{66}Zn-enriched components in the mantle source. The high Zn/Fe ratios of our samples suggest that such non-peridotitic components may comprise recycled oceanic crust in the form of eclogites or garnet pyroxenites (Figure 3a, Le Roux et al., 2010), probably complemented by subducted carbonates (Liu et al., 2016; Xu et al., 2022). However, the observed high δ^{66}Zn values are best ascribed to the putative subducted carbonates with an average value of +0.91 ± 0.54‰ (n = 171), because mid-ocean ridge basalt (MORB; +0.27 ± 0.07‰, n = 61), altered oceanic crust (AOC; +0.27 ± 0.17‰, n = 49) and basaltic eclogites (+0.27 ± 0.08‰, n = 9) have similarly low δ^{66}Zn (Figure 2), and evidence for systematic Zn isotope fractionation during basaltic oceanic crust subduction is lacking (Inglis et al., 2017). Carbonates are only a very minor component of oceanic crust; however, deeply subducted carbonate species can possess very high Zn contents of up to 450 ppm for magnesite and 130 ppm for dolomite (the average Zn concentration of the mantle is 55 ppm) (Liu et al., 2022). Recent Zn isotope studies (e.g., leaching experiments) also suggest that substantial amounts of carbonates may survive beyond subarc mantle depths during slab subduction and potentially be transferred into the deep upper mantle (Qu et al., 2022, 2023). Based on δ^{66}Zn−^{87}Sr/^{86}Sr modeling (Figure S7 in Supporting Information S1), we show that recycled surficial carbonates in the mantle source of the Tarim basalts are dominated by magnesian varieties such as magnesite and dolomite. Negative correlation between δ^{66}Zn and SiO_2 bolsters our argument for high-δ^{66}Zn carbonates in the mantle source (Figure S8 in Supporting Information S1), where they probably were involved in metasomatic reactions by which asthenospheric peridotites in the vicinity of a slab–mantle interface became re-enriched (Zhang et al., 2022). Consequently, melting of recycled oceanic crust together with carbonates would generate carbonated silicate melts, which inherit the high Zn/Fe ratios from recycled oceanic crust and also elevated δ^{66}Zn values from recycled carbonates.

Unlike the exclusively high δ^{66}Zn signature, the Tarim basalts exhibit more variable δ^{98}Mo compositions (−0.39 to +0.27‰) compared to values for the normal mantle (−0.20 ± 0.01‰) (Figure 2). Large δ^{98}Mo variations have been reported for arc lavas, where such signatures are commonly attributed to the diverse inputs of slab-derived fluids (Freymuth et al., 2015). The heavy Mo isotopic compositions of arc lavas are commonly attributed to addition of slab-derived aqueous fluids to their subarc mantle sources, whereas low δ^{98}Mo values are typically interpreted as contributions from subducted sediments including melt components (Fang et al., 2023; König et al., 2016). A notable feature of the intraplate basalts from both western and eastern China is that their δ^{98}Mo compositions are highly correlated with Mo/Ce ratios (Figure 3b). This implies that the observed δ^{98}Mo variations can be explained by a two-component mixing model between an endmember that has low δ^{98}Mo and low Mo/Ce and an endmember that has high δ^{98}Mo and high Mo/Ce. Because Mo is a fluid-mobile element, fluids in subduction zones will preferentially incorporate isotopically heavy Mo during slab dehydration, creating residual recycled oceanic crust that is enriched in isotopically light Mo (Freymuth et al., 2015). Such Mo isotope fractionation has been demonstrated by studies of MORB-type eclogites, which exhibit very low δ^{98}Mo (−0.51 ± 0.44‰, n = 20), low Mo contents (0.04–0.49 ppm, mean = 0.14 ppm, n = 20) and low Mo/Ce ratios (0.001–0.031, mean = 0.01, n = 20) (Figure 2, Chen et al., 2019; Ahmad et al., 2021). Hence, the low δ^{98}Mo and low Mo/Ce endmember most likely represents dehydrated subducted oceanic crust, which is consistent with the trend toward low δ^{98}Mo MORB-type eclogites as approached by our continental basalt samples (Figure 3b). Although incorporation of siliciclastic sediments could cause heavy Mo isotopic compositions, the paired δ^{66}Zn compositions exclude an involvement of recycled silicate-rich sediments in the mantle source (Figure 2). Surficial

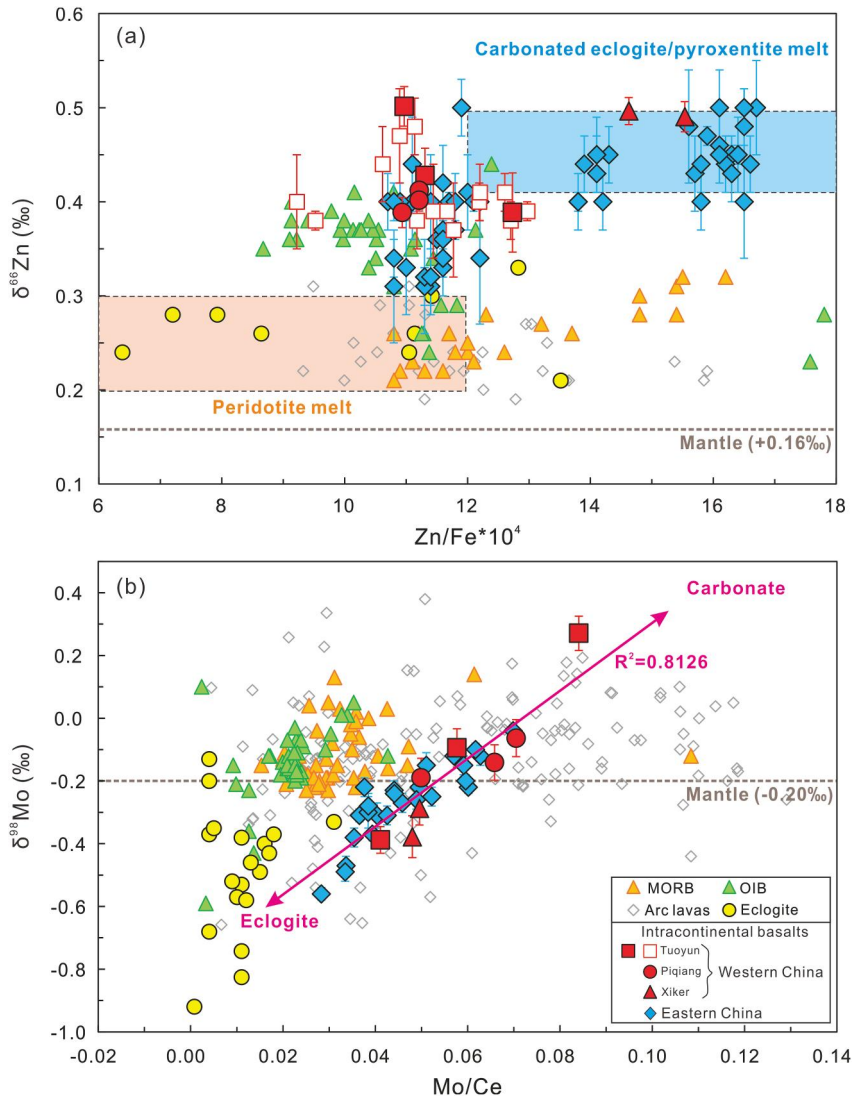

Figure 3. Plots of (a) δ^{66}Zn versus Zn/Fe*10^4 and (b) δ^{98}Mo versus Mo/Ce for Cenozoic basalts from western and eastern China. The data sources are the same as in Figure 2. The Zn/Fe ranges of carbonated eclogite/pyroxenite and peridotite melts are from Le Roux et al. (2010), X. J. Wang et al. (2018), and Z. Z. Wang et al. (2018).

carbonates, characterized by high δ^{98}Mo (+1.66 ± 1.02‰, n = 62), high Mo contents (up to 27.7 ppm) and high Mo/Ce ratios (up to 1.23) (Figure 2, Hoernle et al., 2002; Romaniello et al., 2016), could potentially explain the high δ^{98}Mo signatures of the Tarim basalts. Li et al. (2019) proposed that high δ^{98}Mo signatures of basalts from eastern China indicate the presence of carbonate-rich fluids in their mantle sources. Although it cannot be ruled out that slab dehydration at subarc depths causes removal of calcium carbonates due to their strong fluid solubility, the less soluble Mg-rich carbonates, which are stable at high P-T conditions, can be retained in dehydrated oceanic crust and transported all the way into the deep upper mantle (Shen et al., 2018). Thus, a melting model for the Tarim basalts that invokes contributions from dehydrated oceanic crust (low δ^{98}Mo) and Mg-rich carbonates (high δ^{98}Mo) can reconcile the observed variations in the δ^{98}Mo data, and it can also explain the heavy δ^{66}Zn compositions (Figure 3).

The combined δ^{66}Zn–δ^{98}Mo evidence presented here suggests that intraplate alkali basalts are sourced from upper mantle domains that have been refertilized not only by subducted oceanic crustal components but also by components derived from recycled carbonates. Additional evidence for involvement of recycled carbonates in the metasomatic enrichment of Earth's upper mantle includes: (a) similarities between the Tarim basalts and experimentally produced partial melts of carbonated eclogite (Figure S9 in Supporting Information S1), (b)

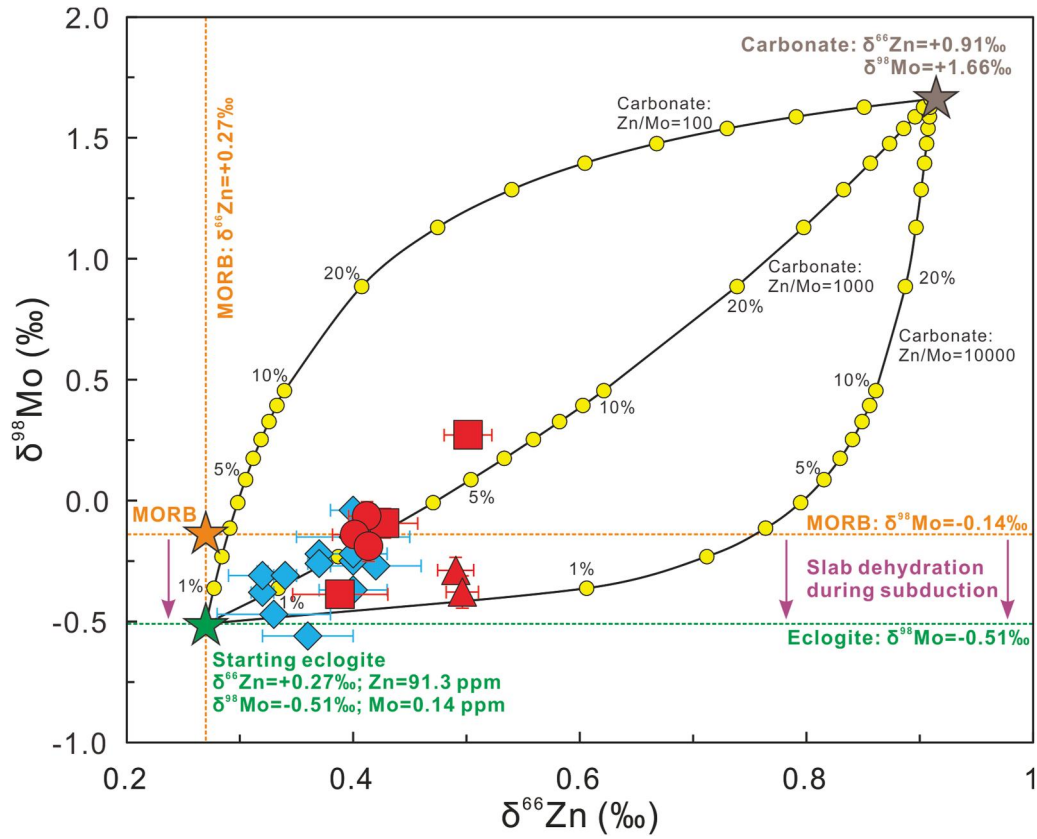

Figure 4. A plot of δ^{66}Zn versus δ^{98}Mo for Cenozoic basalts from western and eastern China, together with mixing cruves between dehydrated oceanic crust (eclogite) and surficial carbonates. The data sources are the same as in Figure 2. Modeling reveals that involvement of ≤5% carbonate-bearing oceanic crust fully resolves the observed δ^{66}Zn–δ^{98}Mo mantle heterogeneity probed by intracontinental basalts. See Supporting Information S1 for details about the compositions of the endmembers and mixing calculation.

negative Zr-Hf-Ti anomalies in mantle-normalized incompatible element patterns (Figure S3 in Supporting Information S1, Tappe et al., 2017; Zhang et al., 2017; Zeng et al., 2010; Zou et al., 2022), and (c) light δ^{26} Mg signatures of the alkali basalts (δ^{26} Mg from −0.55 to −0.45‰, Cheng et al., 2022) given that carbonates have much lower δ^{26} Mg values than normal mantle ($\delta^{26}Mg_{carbonate}$ from −3 to −1‰; $\delta^{26}Mg_{mantle} = -0.25 \pm 0.04$‰) (Liu et al., 2022).

Modeling in δ^{66}Zn–δ^{98}Mo space suggests that only ≤5% of metasomatic components sourced from dehydrated subducted oceanic crust (eclogite) and associated recycled Mg-rich carbonates are required to precondition the peridotitic upper mantle sources of intraplate alkali basalts (Figure 4). Experiments suggest that subducted carbonate-bearing oceanic crust will partially melt and release metasomatizing carbonated silicate melts near the top of the mantle transition zone (MTZ) at about 300–400 km depths (Dasgupta et al., 2004), which is consistent with geophysical evidence showing low-velocity seismic anomalies at deep upper mantle depths beneath the Tarim Craton (Figure 1c).

4. Implications for the Deep Carbon Cycle

The model in Figure 5 depicts the fate of subducted sedimentary carbonates as tracked by combined Zn–Mo isotope evidence from mantle-derived basalts. Subduction introduces oceanic lithosphere and surficial carbonates into Earth's interior. At subarc mantle depths, subducted oceanic crust undergoes dehydration and Ca-rich carbonates are preferentially dissolved in slab-derived fluids, with subsequent release of this portion of the deep carbon inventory to arc volcanism, characterized by heavy δ^{98}Mo magmatic products. The absence of high-δ^{66}Zn signatures in arc magmas is owed to the low Zn content of calcite (mean = 20 ppm), resulting in significant dilution of the Zn isotopic fingerprint of recycled carbonates in the subarc mantle (Liu et al., 2022). As subduction

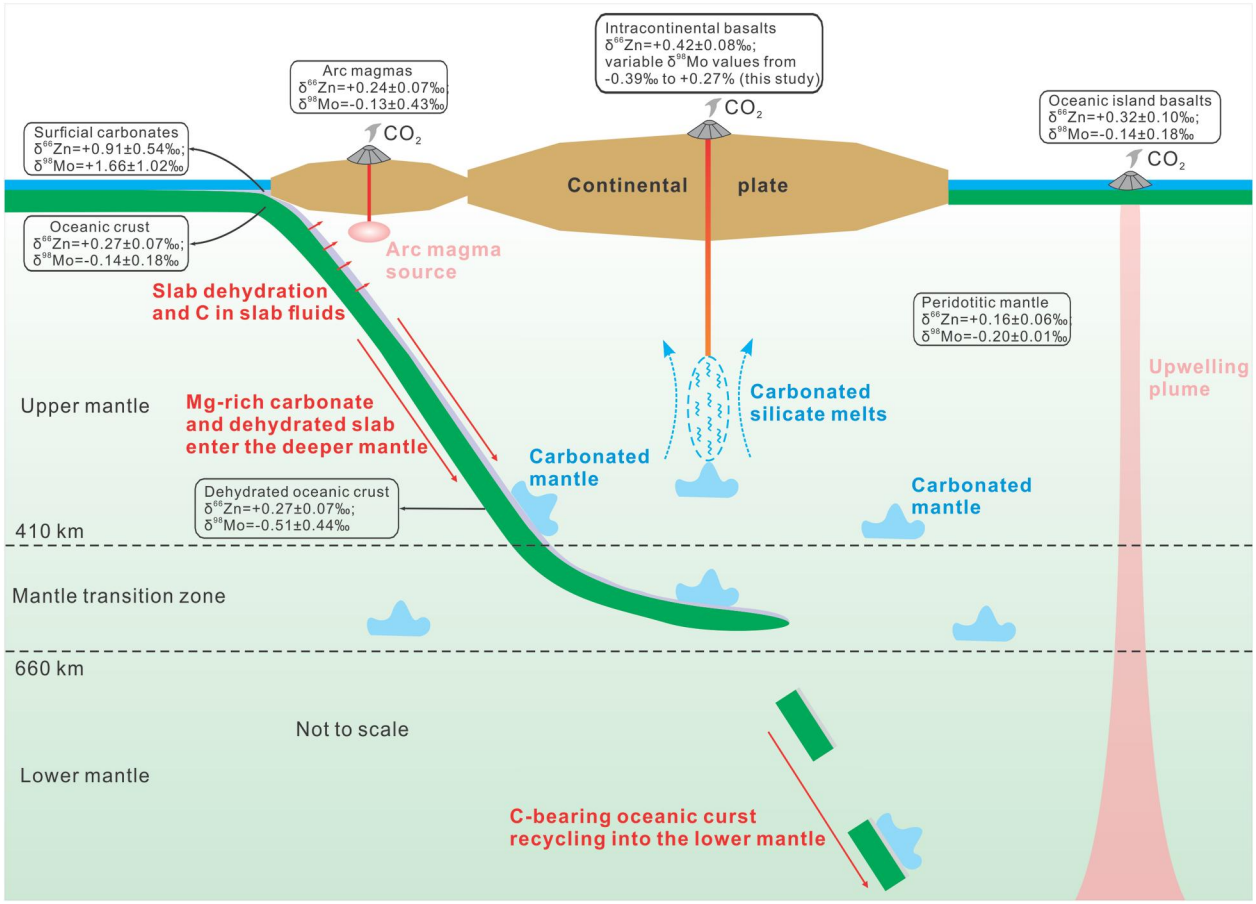

Figure 5. A schematic diagram describing the fate of subducted sedimentary carbonates as tracked by combined Zn-Mo isotope evidence from mantle-derived magmas (see text for details).

proceeds, dehydrated oceanic crust including refractory Mg-rich carbonates is pulled into the deep upper mantle to the top of the MTZ, where carbonated silicate melts with high δ^{66}Zn and variable δ^{98}Mo are released from the slab and metasomatize the surrounding mantle. Such refertilized mantle domains provide potent sources for geochemically enriched basaltic intraplate volcanism. A small fraction of refractory carbonate-bearing oceanic lithosphere may enter the lower mantle and this deep carbon may return to Earth's surface via mantle plume activity (Beunon et al., 2020; Tappe et al., 2020; Zhang et al., 2022).

An important finding of our study is that the Zn–Mo isotopic compositions of Cenozoic intraplate alkali basalts from western China record ≤5% carbonate-bearing oceanic crust components in their deep upper mantle source, which provides indirect evidence for subduction recycling of Mg-rich crustal carbonates beyond subarc mantle depths. Pb isotope modeling of the Cenozoic Tarim basalts indicates formation of the recycled components at ca. 500 Ma (Figure S4 in Supporting Information S1), implying that such geochemically enriched crustal materials do not readily homogenize with the convecting upper mantle and retain part of their identity as long-lived mantle heterogeneities. Recent findings from the petrology of Cenozoic Bermuda basalts in the Central Atlantic suggest that these melts were derived from a carbon-rich source in the MTZ formed <650 Ma ago (Mazza et al., 2019), which supports our carbon-recycling model based on the δ^{66}Zn–δ^{98}Mo systematics of Cenozoic basalts from central Asia. Although several petrology and non-traditional stable metal isotope studies on OIBs (e.g., Cook–Austral, St. Helena, Pitcairn) suggested that subducted crustal carbonates can enter into the lower mantle, all the way down to the core–mantle boundary, where they may isolate for billions of years (X. J. Wang et al., 2018; Z. Z. Wang et al., 2018; Weiss et al., 2016; Zhang et al., 2022), combined δ^{66}Zn–δ^{98}Mo analyses await to be carried out on such plume-sourced lavas to further explore the deepest extension of the geological carbon cycle.

5. Conclusions

We present the first combined high-precision Zn and Mo isotope data for Cenozoic intraplate basalts from western China with the aim to track subducted carbonates in Earth's mantle. The basalts show exceptionally high δ^{66}Zn values (+0.39 to +0.50‰) and variable δ^{98}Mo compositions (−0.39 to +0.27‰), indicating that the mantle source has been refertilized not only by subducted oceanic crustal components but also by components derived from recycled sedimentary carbonates. Modeling reveals that involvement of ≤5% carbonate-bearing oceanic crust fully resolves the observed δ^{66}Zn–δ^{98}Mo mantle heterogeneity probed by intracontinental basalts. Our findings provide new evidence that surficial carbonates can be delivered into the deep upper mantle, highlighting the importance of subduction-driven geological carbon cycling.

Data Availability Statement

The data in Table S4 in Supporting Information is from Gale et al. (2013) and Liu et al. (2016). The data reported in this paper, including Figures S1 to S9 and Tables S1 to S4 in Supporting Information S1, are available in the Mendeley Data repository (Wang, 2023).

Acknowledgments
We are grateful to the editor (Quentin Williams) and reviewer Sarah Mazza and an anonymous peer for their highly constructive criticism. This study was supported by the Second Tibetan Plateau Scientific Expedition and Research Program (STEP) (2019QZKK0702), the Xinjiang Major Science and Technology project (202101679), the National Natural Science Foundation of China (Grants 42203017, 42021002, and 41973033), and the China Postdoctoral Science Foundation (2022M710147). This is contribution No. IS-3470 from GIGCAS. ST thanks the Faculty of Science and Technology at UiT for support of research on Solid Earth topics.

References

Ahmad, Q., Wille, M., König, S., Rosca, C., Hensel, A., Pettke, T., & Hermann, J. (2021). The molybdenum isotope subduction recycling conundrum: A case study from the Tongan subduction zone, western Alps and Alpine Corsica. *Chemical Geology*, *576*, 120231. https://doi.org/10.1016/j.chemgeo.2021.120231

Beunon, H., Mattielli, N., Doucet, L. S., Moine, B., & Debret, B. (2020). Mantle heterogeneity through Zn systematics in oceanic basalts: Evidence for a deep carbon cycling. *Earth-Science Reviews*, *205*, 103174. https://doi.org/10.1016/j.earscirev.2020.103174

Bezard, R., Fischer-Gödde, M., Hamelin, C., Brennecka, G. A., & Kleine, T. (2016). The effects of magmatic processes and crustal recycling on the molybdenum stable isotopic composition of Mid-Ocean Ridge Basalts. *Earth and Planetary Science Letters*, *453*, 171–181. https://doi.org/10.1016/j.epsl.2016.07.056

Chen, H., Savage, P. S., Teng, F.-Z., Helz, R. T., & Moynier, F. (2013). Zinc isotope fractionation during magmatic differentiation and the isotopic composition of the bulk Earth. *Earth and Planetary Science Letters*, *369−370*, 34–42. https://doi.org/10.1016/j.epsl.2013.02.037

Chen, S., Hin, R. C., John, T., Brooker, R., Bryan, B., Niu, Y., & Elliott, T. (2019). Molybdenum systematics of subducted crust record reactive fluid flow from underlying slab serpentine dehydration. *Nature Communications*, *10*(1), 4773. https://doi.org/10.1038/s41467-019-12696-3

Chen, S., Sun, P., Niu, Y., Guo, P., Elliott, T., & Hin, R. C. (2022). Molybdenum isotope systematics of lavas from the East Pacific Rise: Constraints on the source of enriched mid-ocean ridge basalt. *Earth and Planetary Science Letters*, *578*, 117283. https://doi.org/10.1016/j.epsl.2021.117283

Cheng, Z. G., Zhang, Z. C., Wang, Z. C., Jin, Z. L., Hao, J. H., Jin, L., & Santosh, M. (2022). Petrogenesis of continental intraplate alkaline basalts in the Tuoyun basin, western Central Asian orogenic belt. Implications for deep carbon recycling. *Journal of Petrology*, *63*, 1–27. https://doi.org/10.1093/petrology/egac088

Dasgupta, R., Hirschmann, M. M., & Withers, A. C. (2004). Deep global cycling of carbon constrained by the solidus of anhydrous, carbonated eclogite under upper mantle conditions. *Earth and Planetary Science Letters*, *227*(1–2), 73–85. https://doi.org/10.1016/j.epsl.2004.08.004

Day, J. M. D., Moynier, F., & Ishizuka, O. (2022). A partial melting control on the Zn isotope composition of basalts. *Geochemical Perspectives Letters*, *23*, 11–16. https://doi.org/10.7185/geochemlet.2230

Deines, P. (2002). The carbon isotope geochemistry of mantle xenoliths. *Earth-Science Reviews*, *58*(3–4), 247–248. https://doi.org/10.1016/S0012-8252(02)00064-8

Doucet, L. S., Mattielli, N., Ionov, D. A., Debouge, W., & Golovin, A. V. (2016). Zn isotopic heterogeneity in the mantle: A melting control? *Earth and Planetary Science Letters*, *451*, 232–240. https://doi.org/10.1016/j.epsl.2016.06.040

Fang, W., Dai, L.-Q., Zheng, Y.-F., & Zhao, Z.-F. (2023). Molybdenum isotopes in mafic igneous rocks record slabmantle interactions from subarc to postarc depths. *Geology*, *51*(1), 3–7. https://doi.org/10.1130/G50456.1

Freymuth, H., Elliott, T., van Soest, M., & Skora, S. (2016). Tracing subducted black shales in the Lesser Antilles arc using molybdenum isotope ratios. *Geology*, *44*(12), 987–990. https://doi.org/10.1130/G38344.1

Freymuth, H., Vils, F., Willbold, M., Taylor, R. N., & Elliott, T. (2015). Molybdenum mobility and isotopic fractionation during subduction at the Mariana arc. *Earth and Planetary Science Letters*, *432*, 176–186. https://doi.org/10.1016/j.epsl.2015.10.006

Gale, A., Dalton, C. A., Langmuir, C. H., Su, Y., & Schilling, J.-G. (2013). The mean composition of ocean ridge basalts. *Geochemistry, Geophysics, Geosystems*, *14*(3), 489–518. https://doi.org/10.1029/2012GC004334

Gaschnig, R. M., Rader, S. T., Reinhard, C. T., Owens, J. D., Planavsky, N., Wang, X., et al. (2021). Behavior of the Mo, Tl, and U isotope systems during differentiation in the Kilauea Iki lava lake. *Chemical Geology*, *574*, 120239. https://doi.org/10.1016/j.chemgeo.2021.120239

Gaschnig, R. M., Reinhard, C. T., Planavsky, N. J., Wang, X., Asael, D., & Chauvel, C. (2017). The molybdenum isotope system as a tracer of slab input in subduction zones: An example from Martinique, Lesser Antilles Arc. *Geochemistry, Geophysics, Geosystems*, *18*(12), 4674–4689. https://doi.org/10.1002/2017GC007085

Hoernle, K., Tilton, G., Le Bas, M. J., Duggen, S., & Garbe-Schonberg, D. (2002). Geochemistry of oceanic carbonatites compared with continental carbonatites: Mantle recycling of oceanic crustal carbonate. *Contributions to Mineralogy and Petrology*, *142*(5), 520–542. https://doi.org/10.1007/s004100100308

Huang, J., Liu, S.-A., Gao, Y., Xiao, Y., & Chen, S. (2016). Copper and zinc isotope systematics of altered oceanic crust at IODP Site 1256 in the eastern equatorial Pacific. *Journal of Geophysical Research: Solid Earth*, *121*(10), 7086–7100. https://doi.org/10.1002/2016JB013095

Huang, J., Zhang, X.-C., Chen, S., Tang, L., Wörner, G., Yu, H., & Huang, F. (2018). Zinc isotopic systematics of Kamchatka-Aleutian arc magmas controlled by mantle melting. *Geochimica et Cosmochimica Acta*, *238*, 85–101. https://doi.org/10.1016/j.gca.2018.07.012

Huang, J. L., & Zhao, D. P. (2006). High-resolution mantle tomography of China and surrounding regions. *Journal of Geophysical Research*, *111*(B9), B09305. https://doi.org/10.1029/2005JB004066

Inglis, E. C., Debret, B., Burton, K. W., Millet, M.-A., Pons, M.-L., Dale, C. W., et al. (2017). The behavior of iron and zinc stable isotopes accompanying the subduction of mafic oceanic crust: A case study from western Alpine ophiolites. *Geochemistry, Geophysics, Geosystems*, *18*(7), 2562–2579. https://doi.org/10.1002/2016GC006735

Kelemen, B., & Manning, C. E. (2015). Reevaluating carbon fluxes in subduction zones, what goes down, mostly comes up. *Proceedings of the National Academy of Sciences of the United States of America*, *112*(30), 3997–4006. https://doi.org/10.1073/pnas.1507889112

König, S., Wille, M., Voegelin, A., & Schoenberg, R. (2016). Molybdenum isotope systematics in subduction zones. *Earth and Planetary Science Letters*, *447*, 95–102. https://doi.org/10.1016/j.epsl.2016.04.033

Le Roux, V., Lee, C. T. A., & Turner, S. J. (2010). Zn/Fe systematics in mafic and ultramafic systems: Implications for detecting major element heterogeneities in the Earth's mantle. *Geochimica et Cosmochimica Acta*, *74*(9), 2779–2796. https://doi.org/10.1016/j.gca.2010.02.004

Li, H.-Y., Li, J., Ryan, J. G., Li, X., Zhao, R.-P., Ma, L., & Xu, Y.-G. (2019). Molybdenum and boron isotope evidence for fluid-fluxed melting of intraplate upper mantle beneath the eastern North China Craton. *Earth and Planetary Science Letters*, *520*, 105–114. https://doi.org/10.1016/j.epsl.2019.05.038

Li, H. Y., Zhao, R. P., Li, J., Tamura, Y., Spencer, C., Stern, R. J., et al. (2021). Molybdenum isotopes unmask slab dehydration and melting beneath the Mariana arc. *Nature Communications*, *12*(1), 6015. https://doi.org/10.1038/s41467-021-26322-8

Li, X., Yan, Q., Zeng, Z., Fan, J., Li, S., Li, J., et al. (2021b). Across-arc variations in Mo isotopes and implications for subducted oceanic crust in the source of back-arc basin volcanic rocks. *Geology*, *49*(10), 1165–1170. https://doi.org/10.1130/G48754.1

Liang, Y.-H., Halliday, A. N., Siebert, C., Fitton, J. G., Burton, K. W., Wang, K.-L., & Harvey, J. (2017). Molybdenum isotope fractionation in the mantle. *Geochimica et Cosmochimica Acta*, *199*, 91–111. https://doi.org/10.1016/j.gca.2016.11.023

Lin, Z., Sun, X., Strauss, H., Eroglu, S., Böttcher, M. E., Lu, Y., et al. (2021). Molybdenum isotope composition of seep carbonates – Constraints on sediment biogeochemistry in seepage environments. *Geochimica et Cosmochimica Acta*, *307*, 56–71. https://doi.org/10.1016/j.gca.2021.05.038

Little, S. H., Vance, D., McManus, J., & Severmann, S. (2016). Key role of continental margin sediments in the oceanic mass balance of Zn and Zn isotopes. *Geology*, *44*(3), 207–210. https://doi.org/10.1130/G37493.1

Liu, S.-A., Qu, Y.-R., Wang, Z.-Z., Li, M.-L., Yang, C., & Li, S.-G. (2022). The fate of subducting carbon tracked by Mg and Zn isotopes: A review and new perspectives. *Earth-Science Reviews*, *228*, 104010. https://doi.org/10.1016/j.earscirev.2022.104010

Liu, S.-A., Wang, Z.-Z., Li, S.-G., Huang, J., & Yang, W. (2016). Zinc isotope evidence for a large-scale carbonated mantle beneath eastern China. *Earth and Planetary Science Letters*, *444*, 169–178. https://doi.org/10.1016/j.epsl.2016.03.051

Liu, S.-A., Wu, H., Shen, S.-Z., Jiang, G., Zhang, S., Lv, Y., et al. (2017). Zinc isotope evidence for intensive magmatism immediately before the end-Permian mass extinction. *Geology*, *45*(4), 343–346. https://doi.org/10.1130/G38644.1

Maréchal, C. N., Nicolas, E., Douchet, C., & Albarède, F. (2000). Abundance of zinc isotopes as a marine biogeochemical tracer. *Geochemistry, Geophysics, Geosystems*, *1*(5), 1015. https://doi.org/10.1029/1999GC000029

Mazza, S. E., Gazel, E., Bizimis, M., Moucha, R., Beguelin, P., Johnson, E. A., et al. (2019). Sampling the volatile-rich transition zone beneath Bermuda. *Nature*, *569*(7756), 398–403. https://doi.org/10.1038/s41586-019-1183-6

McCoy-West, A. J., Chowdhury, P., Burton, K. W., Sossi, P., Nowell, G. M., Fitton, J. G., et al. (2019). Extensive crustal extraction in Earth's early history inferred from molybdenum isotopes. *Nature Geoscience*, *12*(11), 946–951. https://doi.org/10.1038/s41561-019-0451-2

Pichat, S., Douchet, C., & Albarède, F. (2003). Zinc isotope variations in deep-sea carbonates from the eastern equatorial Pacific over the last 175 ka. *Earth and Planetary Science Letters*, *210*(1–2), 167–178. https://doi.org/10.1016/S0012-821X(03)00106-7

Pickard, H., Palk, E., Schönbächler, M., Moore, R. E. T., Coles, B. J., Kreissig, K., et al. (2022). The cadmium and zinc isotope compositions of the silicate Earth – Implications for terrestrial volatile accretion. *Geochimica et Cosmochimica Acta*, *338*, 165–180. https://doi.org/10.1016/j.gca.2022.09.041

Qu, Y.-R., Liu, S.-A., Busigny, V., Wang, Z.-Z., & Teng, F.-Z. (2023). Carbonate-silicate interaction in subducting slabs recorded by Zn isotopes in western Alps metasediments. *Earth and Planetary Science Letters*, *616*, 118234. https://doi.org/10.1016/j.epsl.2023.118234

Qu, Y.-R., Liu, S.-A., Wu, H., Li, M.-L., & Tian, H.-C. (2022). Tracing carbonate dissolution in subducting sediments by zinc and magnesium isotopes. *Geochimica et Cosmochimica Acta*, *319*, 56–72. https://doi.org/10.1016/j.gca.2021.12.020

Romaniello, S. J., Herrmann, A. D., & Anbar, A. D. (2016). Syndepositional diagenetic control of molybdenum isotope variations in carbonate sediments from the Bahamas. *Chemical Geology*, *438*, 84–90. https://doi.org/10.1016/j.chemgeo.2016.05.019

Shen, J., Li, S.-G., Wang, S.-J., Teng, F.-Z., Li, Q.-L., & Liu, Y.-S. (2018). Subducted Mg-rich carbonates into the deep mantle wedge. *Earth and Planetary Science Letters*, *503*, 118–130. https://doi.org/10.1016/j.epsl.2018.09.011

Smart, K. A., Chacko, T., Stachel, T., Muehlenbachs, K., Stern, R. A., & Heaman, L. M. (2011). Diamond growth from oxidized carbon sources beneath the Northern Slave Craton, Canada: A δ^{13}C–N study of eclogite-hosted diamonds from the Jericho kimberlite. *Geochimica et Cosmochimica Acta*, *75*(20), 6027–6047. https://doi.org/10.1016/j.gca.2011.07.028

Smith, E. M., Shirey, S. B., Richardson, S. H., Nestola, F., Bullock, E. S., Wang, J., & Wang, W. (2018). Blue boron-bearing diamonds from Earth's lower mantle. *Nature*, *560*(7716), 84–87. https://doi.org/10.1038/s41586-018-0334-5

Sonke, J., Sivry, Y., Viers, J., Freydier, R., Dejonghe, L., André, L., et al. (2008). Historical variations in the isotopic composition of atmospheric zinc deposition from a zinc smelter. *Chemical Geology*, *252*(3–4), 145–157. https://doi.org/10.1016/j.chemgeo.2008.02.006

Sossi, A., Nebel, O., O'Neill, H. S. C., & Moynier, F. (2018). Zinc isotope composition of the Earth and its behaviour during planetary accretion. *Chemical Geology*, *477*, 73–84. https://doi.org/10.1016/j.chemgeo.2017.12.006

Sun, P., Niu, Y., Duan, M., Chen, S., Guo, P., Gong, H., et al. (2023). Zinc isotope fractionation during mid-ocean ridge basalt differentiation: Evidence from lavas on the East Pacific Rise at 10°30'N. *Geochimica et Cosmochimica Acta*, *346*, 180–191. https://doi.org/10.1016/j.gca.2023.02.012

Sweere, T. C., Dickson, A. J., Jenkyns, H. C., Porcelli, D., Elrick, M., van den Boorn, S. H. J. M., & Henderson, G. M. (2018). Isotopic evidence for changes in the zinc cycle during oceanic anoxic event 2 (late cretaceous). *Geology*, *46*(5), 463–466. https://doi.org/10.1130/G40226.1

Tappe, S., Budde, G., Stracke, A., Wilson, A., & Kleine, T. (2020). The tungsten-182 record of kimberlites above the African superplume: Exploring links to the core-mantle boundary. *Earth and Planetary Science Letters*, *547*, 116473. https://doi.org/10.1016/j.epsl.2020.116473

Tappe, S., Romer, R. L., Stracke, A., Steenfelt, A., Smart, K. A., Muehlenbachs, K., & Torsvik, T. H. (2017). Sources and mobility of carbonate melts beneath cratons, with implications for deep carbon cycling, metasomatism and rift initiation. *Earth and Planetary Science Letters*, *466*, 152–167. https://doi.org/10.1016/j.epsl.2017.03.011

Vance, D., Little, S. H., Archer, C., Cameron, V., Andersen, M. B., Rijkenberg, M. J. A., & Lyons, T. W. (2016). The oceanic budgets of nickel and zinc isotopes: The importance of sulfidic environments as illustrated by the Black Sea. *Philosophical Transactions: Mathematical, Physical and Engineering Sciences*, *374*(2081), 20150294. https://doi.org/10.1098/rsta.2015.0294

Villalobos-Orchard, J., Freymuth, H., O'Driscoll, B., Elliott, T., Williams, H., Casalini, M., & Willbold, M. (2020). Molybdenum isotope ratios in Izu arc basalts: The control of subduction zone fluids on compositional variations in arc volcanic systems. *Geochimica et Cosmochimica Acta*, *288*, 68–82. https://doi.org/10.1016/j.gca.2020.07.043

Voegelin, A. R., Nägler, T. F., Samankassou, E., & Villa, I. M. (2009). Molybdenum isotopic composition of modern and Carboniferous carbonates. *Chemical Geology*, *265*(3–4), 488–498. https://doi.org/10.1016/j.chemgeo.2009.05.015

Walter, M. J., Kohn, S. C., Araujo, D., Bulanova, G. P., Smith, C. B., Gaillou, E., et al. (2011). Deep mantle cycling of oceanic crust: Evidence from diamonds and their mineral inclusions. *Science*, *334*(6052), 54–57. https://doi.org/10.1126/science.1209300

Wang, J. (2023). Tracing subducted carbonates in Earth's mantle using zinc and molybdenum isotopes [Dataset]. Mendeley Data, V4. https://doi.org/10.17632/k6kcgz3ctb

Wang, J., Su, Y., Zheng, J., Dai, H., Tang, G., Ma, Q., et al. (2023). Cenozoic intraplate volcanism in central Asia: Mantle upwelling induced by India-Eurasia collision. *Geological Society of America Bulletin*, *135*, 1923–1938. https://doi.org/10.1130/B36545.1

Wang, X. J., Chen, L. H., Hofmann, A. W., Hanyu, T., Kawabata, H., Zhong, Y., et al. (2018). Recycled ancient ghost carbonate in the Pitcairn mantle plume. *Proceedings of the National Academy of Sciences of the United States of America*, *115*(35), 8682–8687. https://doi.org/10.1073/pnas.1719570115

Wang, Z.-Z., Liu, S.-A., Chen, L.-H., Li, S.-G., & Zeng, G. (2018). Compositional transition in natural alkaline lavas through silica-undersaturated melt–lithosphere interaction. *Geology*, *46*(9), 771–774. https://doi.org/10.1130/G45145.1

Wang, Z.-Z., Liu, S.-A., Liu, J., Huang, J., Xiao, Y., Chu, Z.-Y., et al. (2017). Zinc isotope fractionation during mantle melting and constraints on the Zn isotope composition of Earth's upper mantle. *Geochimica et Cosmochimica Acta*, *198*, 151–167. https://doi.org/10.1016/j.gca.2016.11.014

Weiss, Y., Class, C., Goldstein, S. L., & Hanyu, T. (2016). Key new pieces of the HIMU puzzle from olivines and diamond inclusions. *Nature*, *537*(7622), 666–670. https://doi.org/10.1038/nature19113

Xu, R., Liu, Y., Lambart, S., Hoernle, K., Zhu, Y., Zou, Z., et al. (2022). Decoupled Zn-Sr-Nd isotopic composition of continental intraplate basalts caused by two-stage melting process. *Geochimica et Cosmochimica Acta*, *326*, 234–252. https://doi.org/10.1016/j.gca.2022.03.014

Yang, J., Siebert, C., Barling, J., Savage, P., Liang, Y.-H., & Halliday, A. N. (2015). Absence of molybdenum isotope fractionation during magmatic differentiation at Hekla volcano, Iceland. *Geochimica et Cosmochimica Acta*, *162*, 126–136. https://doi.org/10.1016/j.gca.2015.04.011

Yu, Y., Huang, X.-L., Chung, S.-L., Li, J., Lai, Y.-M., Setiawan, I., & Sun, M. (2022). Molybdenum isotopic constraint from Java on slab inputs to subduction zone magmatism. *Geochimica et Cosmochimica Acta*, *332*, 1–18. https://doi.org/10.1016/j.gca.2022.06.009

Zeng, G., Chen, L.-H., Xu, X.-S., Jiang, S.-Y., & Hofmann, A. W. (2010). Carbonated mantle sources for Cenozoic intra-plate alkaline basalts in Shandong, North China. *Chemical Geology*, *273*(1–2), 35–45. https://doi.org/10.1016/j.chemgeo.2010.02.009

Zhang, G. L., Chen, L. H., Jackson, M. G., & Hofmann, A. W. (2017). Evolution of carbonated melt to alkali basalt in the South China Sea. *Nature Geoscience*, *10*(3), 229–235. https://doi.org/10.1038/ngeo2877

Zhang, X. Y., Chen, L. H., Wang, X. J., Hanyu, T., Hofmann, A. W., Komiya, T., et al. (2022). Zinc isotopic evidence for recycled carbonate in the deep mantle. *Nature Communications*, *13*(1), 6085. https://doi.org/10.1038/s41467-022-33789-6

Zhang, Y., Yuan, C., Sun, M., Li, J., Long, X., Jiang, Y., & Huang, Z. (2020). Molybdenum and boron isotopic evidence for carbon-recycling via carbonate dissolution in subduction zones. *Geochimica et Cosmochimica Acta*, *278*, 340–352. https://doi.org/10.1016/j.gca.2019.12.013

Zou, Z., Wang, Z., Foley, S., Xu, R., Geng, X., Liu, Y.-N., et al. (2022). Origin of low-MgO primitive intraplate alkaline basalts from partial melting of carbonate-bearing eclogite sources. *Geochimica et Cosmochimica Acta*, *324*, 240–261. https://doi.org/10.1016/j.gca.2022.02.022

References From the Supporting Information

Baker, J., Peate, D., Waight, T., & Meyzen, C. (2004). Pb isotopic analysis of standards and samples using a ^{207}Pb-^{204}Pb double spike and thallium to correct for mass bias with a double-focusing MC-ICP-MS. *Chemical Geology*, *211*(3–4), 275–303. https://doi.org/10.1016/j.chemgeo.2004.06.030

Chen, S., Liu, Y., Hu, J., Zhang, Z., Hou, Z., Huang, F., & Yu, H. (2016). Zinc isotopic compositions of NIST SRM 683 and whole-rock reference materials. *Geostandards and Geoanalytical Research*, *40*(3), 417–432. https://doi.org/10.1111/j.1751-908X.2015.00377.x

Dasgupta, R., Hirschmann, M. M., & Stalker, K. (2006). Immiscible transition from carbonate-rich to silicate-rich melts in the 3 GPa melting interval of eclogite + CO_2 and genesis of silica-undersaturated ocean island lavas. *Journal of Petrology*, *47*(4), 647–671. https://doi.org/10.1093/petrology/egi088

Dasgupta, R., Hirschmann, M. M., & Smith, N. D. (2007). Partial melting experiments of peridotite + CO_2 at 3 GPa and genesis of alkalic ocean island basalts. *Journal of Petrology*, *48*(11), 2093–2124. https://doi.org/10.1093/petrology/egm053

Dasgupta, R., Mallik, A., Tsuno, K., Withers, A. C., Hirth, G., & Hirschmann, M. M. (2013). Carbon-dioxide-rich silicate melt in the Earth's upper mantle. *Nature*, *493*(7431), 211–215. https://doi.org/10.1038/nature11731

Gerbode, C., & Dasgupta, R. (2010). Carbonate-fluxed melting of MORB-like pyroxenite at 2·9 GPa and genesis of HIMU ocean island basalts. *Journal of Petrology*, *51*(10), 2067–2088. https://doi.org/10.1093/petrology/egq049

Hirschmann, M. M., Kogiso, T., Baker, M. B., & Stolper, E. M. (2003). Alkalic magmas generated by partial melting of garnet pyroxenite. *Geology*, *31*(6), 481–484. https://doi.org/10.1130/0091-7613(2003)031%3C0481:AMGBPM%3E2.0.CO;2

Hofmann, A. W., Jochum, K. P., Seufert, M., & White, W. M. (1986). Nb and Pb in oceanic basalts: New constraints on mantle evolution. *Earth and Planetary Science Letters*, *79*(1–2), 33–45. https://doi.org/10.1016/0012-821X(86)90038-5

Keshav, S., Gudfinnsson, G. H., Sen, G., & Fei, Y. (2004). High-pressure melting experiments on garnet clinopyroxenite and the alkalic to tholeiitic transition in ocean-island basalts. *Earth and Planetary Science Letters*, *223*(3–4), 365–379. https://doi.org/10.1016/j.epsl.2004.04.029

Kiseeva, E. S., Yaxley, G. M., Hermann, J., Litasov, K. D., Rosenthal, A., & Kamenetsky, V. S. (2012). An experimental study of carbonated eclogite at 3·5–5·5 GPa: Implications for silicate and carbonate metasomatism in the cratonic mantle. *Journal of Petrology*, *53*(4), 727–759. https://doi.org/10.1093/petrology/egr078

Kogiso, T., & Hirschmann, M. M. (2006). Partial melting experiments of bimineralic eclogite and the role of recycled mafic oceanic crust in the genesis of ocean island basalts. *Earth and Planetary Science Letters*, *249*(3–4), 188–199. https://doi.org/10.1016/j.epsl.2006.07.016

Kogiso, T., Hirschmann, M. M., & Frost, D. J. (2003). High-pressure partial melting of garnet pyroxenite: Possible mafic lithologies in the source of ocean island basalts. *Earth and Planetary Science Letters*, *216*(4), 603–617. https://doi.org/10.1016/S0012-821X(03)00538-7

Lambart, S., Laporte, D., Provost, A., & Schiano, P. (2012). Fate of pyroxenite-derived melts in the peridotitic mantle: Thermodynamic and experimental constraints. *Journal of Petrology*, *53*(3), 451–476. https://doi.org/10.1093/petrology/egr068

Li, J., Liang, X. R., Zhong, L. F., Wang, X. C., Ren, Z. Y., Sun, S. L., et al. (2014). Measurement of the isotopic composition of molybdenum in geological samples by MC-ICP-MS using a novel chromatographic extraction technique. *Geostandards and Geoanalytical Research*, *38*(3), 345–354. https://doi.org/10.1111/j.1751-908X.2013.00279.x

McDonough, W. F., & Sun, S.-S. (1995). The composition of the Earth. *Chemical Geology*, *120*(3–4), 223–253. https://doi.org/10.1016/0009-2541(94)00140-4

Pertermann, M., & Hirschmann, M. M. (2003). Anhydrous partial melting experiments on MORB-like eclogite: Phase relations, phase compositions and mineral-melt partitioning of major elements at 2–3 GPa. *Journal of Petrology*, *44*(12), 2173–2201. https://doi.org/10.1093/petrology/egg074

Pilet, S., Baker, M. B., & Stolper, E. M. (2008). Metasomatized lithosphere and the origin of alkaline lavas. *Science*, *320*(5878), 916–919. https://doi.org/10.1126/science.1156563

Rudnick, R. L., & Gao, S. (2003). Composition of the continental crust. In H. D. Holland & K. K. Turekian (Eds.), *Treatise on geochemistry* (Vol. 3, pp. 1–64). Elsevier.

Spandler, C., Yaxley, G., Green, D. H., & Rosenthal, A. (2008). Phase relations and melting of anhydrous K-bearing eclogite from 1200 to 1600°C and 3 to 5 GPa. *Journal of Petrology*, *49*(4), 771–795. https://doi.org/10.1093/petrology/egm039

Stacey, J. S., & Kramers, J. D. (1975). Approximation of terrestrial lead isotope evolution by a two-stage model. *Earth and Planetary Science Letters*, *26*(2), 207–221. https://doi.org/10.1016/0012-821X(75)90088-6

Sun, S. S., & McDonough, W. F. (1989). Chemical and isotopic systematics of oceanic basalts: Implications for mantle composition and processes. In A. D. Saunders & M. J. Norry (Eds.), *Magmatism in the ocean basins* (Vol. 42, pp. 313–345). Geological Society [London] Special Publication. https://doi.org/10.1144/GSL.SP.1989.042.01.19

Willbold, M., Hibbert, K., Lai, Y. J., Freymuth, H., Hin, R. C., Coath, C., et al. (2016). High-precision mass-dependent molybdenum isotope variations in magmatic rocks determined by double-spike MC-ICP-MS. *Geostandards and Geoanalytical Research*, *40*, 389–403. https://doi.org/10.1111/j.1751-908X.2015.00388.x

Xu, Y.-G., Wei, X., Luo, Z.-Y., Liu, H.-Q., & Cao, J. (2014). The early permian Tarim large igneous province: Main characteristics and a plume incubation model. *Lithos*, *204*, 20–35. https://doi.org/10.1016/j.lithos.2014.02.015

Zhao, G., Wang, Y., Huang, B., Dong, Y., Li, S., Zhang, G., & Yu, S. (2018). Geological reconstructions of the East Asian blocks: From the breakup of Rodinia to the assembly of Pangea. *Earth-Science Reviews*, *186*, 262–286. https://doi.org/10.1016/j.earscirev.2018.10.003

Zhao, P.-P., Li, J., Zhang, L., Wang, Z.-B., Kong, D.-X., Ma, J.-L., et al. (2016). Molybdenum mass fractions and isotopic compositions of international geological reference materials. *Geostandards and Geoanalytical Research*, *40*(2), 217–226. https://doi.org/10.1111/j.1751-908X.2015.00373.x

Zhang, W., & Hu, Z. C. (2020). Estimation of isotopic reference values for pure materials and geological reference materials. *Atomic Spectroscopy*, *41*(3), 93–102. https://doi.org/10.46770/AS.2020.03.001

Zhu, Y.-T., Li, M., Wang, Z.-C., Zou, Z.-Q., Hu, Z.-C., Liu, Y.-S., et al. (2019). High-precision copper and zinc isotopic measurements of igneous rock standards using a large-geometry MC-ICP-MS. *Atomic Spectroscopy*, *40*(6), 206–214. https://doi.org/10.1039/C3JA50232E